Interaction of Frustrated Magnetic Sublattices in $ErMnO_3$

M. Fiebig,[1,*] C. Degenhardt,[1] and R. V. Pisarev[2]

[1]*Universität Dortmund, Institut für Physik, 44221 Dortmund, Germany*

[2]*Ioffe Physical Technical Institute of the Russian Academy of Sciences, 194021 St. Petersburg, Russia*

(Received 29 August 2001; published 27 December 2001)

A spontaneous or field induced "hidden" phase transition with antiferromagnetic-to-ferromagnetic reordering is disclosed in multiply frustrated hexagonal $ErMnO_3$. It is revealed by Faraday rotation and second harmonic generation as sublattice-sensitive probes to the Er and Mn systems. The acquired phase diagram in the magnetic-field–temperature plane is shown to be a consequence of a broken geometric frustration between the Er and Mn lattices, giving way to anisotropic superexchange between the $3d$ and $4f$ ions.

DOI: 10.1103/PhysRevLett.88.027203 PACS numbers: 75.25.+z, 42.65.Ky, 75.30.Et, 78.20.Ls

Phase transitions and critical phenomena of frustrated magnetic systems have been a central issue of statistical physics for many years [1,2]. Because of the extra degree of freedom arising from the degeneracy of its classical ground state, the nature of magnetic phase transitions in a frustrated compound can be entirely different from that of a nonfrustrated compound. In particular, mechanisms lifting the degeneracy determine the phase diagrams and other physical properties. For instance, orbital frustration can lead to insulator-metal transitions [3]. The 120° orientation of spins which overcomes the frustration of a triangular-lattice antiferromagnet can lead to new universality classes of critical exponents with chirality as additional degree of freedom [2,4]. Frustration leads to the development of new, nonperturbative approaches in solid-state theory since perturbative methods fail to describe it [5].

As these examples demonstrate, frustration and its breaking have a strong potential for novel physics. In this Letter, an unusual "hidden" magnetic phase transition is disclosed in multiply frustrated hexagonal $ErMnO_3$. A first-order phase transition of the Mn lattice is obscured by magnetic ordering of the Er lattice and difficult to observe by magnetization measurements. However, it is clearly revealed by Faraday rotation (FR) and second harmonic generation (SHG) which act as sublattice-sensitive probes to the Er and Mn systems. The transition is a consequence of the breaking of geometric frustration in and between the sublattices which gives way to anisotropic superexchange between the $3d$ and $4f$ ions. Although our discussion is limited to the case of $ErMnO_3$, similar behavior was observed in other rare-earth manganites.

With many competing magnetic inter- and intrasublattice interactions, hexagonal $ErMnO_3$ is a strongly correlated system. The ions forming the $Mn^{3+}(3d^4)$ sublattice are all located at 6(c) positions with the local symmetry m. The ions forming the $Er^{3+}(4f^{11})$ sublattice are located at 4(b) and 2(a) positions with the local symmetry 3 and $3m$, respectively [6]. Because of the triangular geometry shown in Fig. 1, frustration occurs not only in but also in between the Mn and Er sublattices since the local magnetic moments of the Mn spins at the positions of the Er ions cancel.

The magnetic ordering of the Mn sublattice is dominated by antiferromagnetic in-plane Mn—O—Mn superexchange and supplemented by a 2 orders of magnitude weaker interplane Mn—O—O—Mn exchange in the

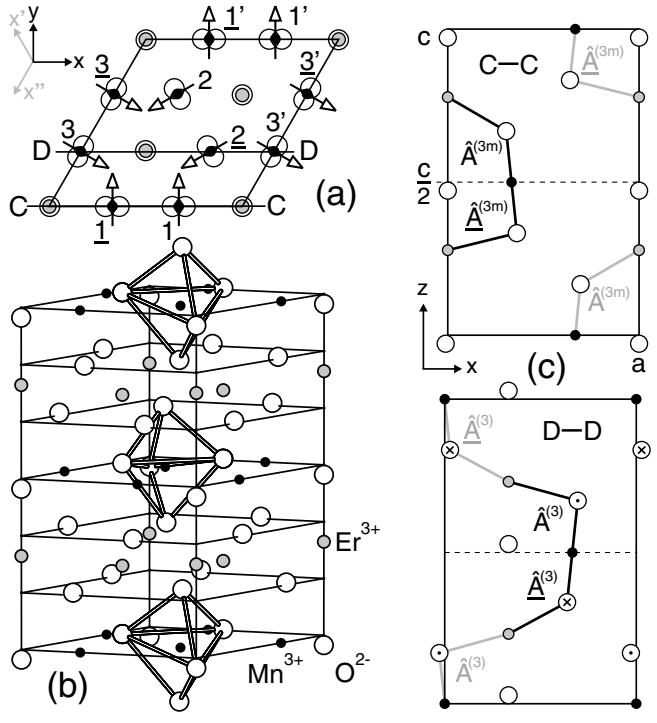

FIG. 1. (a) Top and (b) stereoscopic view of the unit cell of $ErMnO_3$ with Mn spins for antiferromagnetic coupling between planes at 0 and $c/2$. For ferromagnetic coupling the spins labeled with an underbar have to be reversed. (c) Sections showing the dominant contributions to the Mn^{3+}-Er^{3+} superexchange with their exchange matrices $\hat{A}^{3m}$, $\hat{A}^{3}$, $\underline{\hat{A}}^{3m}$, $\underline{\hat{A}}^{3}$. Crosses (dots) denote O ions lying $0.025a$ below ($0.033a$ above) the depicted plane.

stacked triangular lattice [7]. Below $T_N = 79$ K, a 120° arrangement of Mn spins in the basal plane breaks the triangular frustration [8]. The Mn spins orient along the crystallographic y axes with $P\underline{6}_3\underline{c}m$ as magnetic symmetry [9]. Note that the upper and the lower half of the magnetic unit cell can be transformed into each other by the operation $\underline{6}(0, 0, c/2)$, i.e., a rotation by 60° around the hexagonal z axis in combination with time reversal and a translation by half a unit cell along z. The time-reversal operation indicates that the Mn planes at $z = 0$ and $z = c/2$ are coupled antiferromagnetically by the Mn—O—O—Mn exchange [10]. Below 6 K, a weak spontaneous magnetic moment and discontinuities of the dielectric and the magnetoelectric functions indicate ordering of the Er spins [11–13]. However, details of the magnetic structure and interactions of the Er lattice are unknown.

In the experiment, linear and nonlinear magneto-optical techniques were applied. FR couples to a magnetic field $\vec{H}$ or to a sublattice magnetization $\vec{M}$ by

$$P_i(\omega, \vec{k}) = \epsilon_0 \chi^{\mathrm{FR}}_{ijk} B_j(0) E_k(\omega, \vec{k}), \qquad (1)$$

in which the polarization $\vec{P}(\omega, \vec{k})$ induced by $\vec{B} = \mu_0(\vec{H} + \vec{M})$ leads to a rotation of the polarization of the incident light with frequency ω and wave vector $\vec{k}$. Here, the FR from the Mn d-d transitions is employed to monitor the Er ordering.

Further, SHG couples to the magnetic ordering by

$$P_i(2\omega, 2\vec{k}) = \epsilon_0 \chi^{\mathrm{mag}}_{ijk} E_j(\omega, \vec{k}) E_k(\omega, \vec{k}), \qquad (2)$$

where $\vec{E}(\omega, \vec{k})$ and $\vec{P}(2\omega, 2\vec{k})$ represent the incident light at the frequency ω and the polarization induced in the material at the frequency 2ω. The set of nonzero tensor components $\chi^{\mathrm{mag}}_{ijk}$ corresponds to the magnetic structure: The antiferromagnetic coupling between neighboring Mn planes along z leads to $P_\rho(2\omega, 2k_z) \neq 0$ and $P_z(2\omega, 2k_\rho) = 0$ in Eq. (2) (ρ denoting vector components in the xy plane), whereas for ferromagnetic coupling one gets $P_\rho(2\omega, 2k_z) = 0$ and $P_z(2\omega, 2k_\rho) \neq 0$ [9].

The $ErMnO_3$ crystals were grown from the flux or by the floating-zone method and prepared into polished $\sim$100 μm thick z or x oriented platelets, respectively. They were excited with 5 ns light pulses from an optical parametric oscillator with photon energies up to 1.55 eV. The FR was determined from the polarization of the linearly polarized light transmitted through the sample. The total intensity of the SH signal was recorded after suppressing the fundamental light wave with optical filters. A charge-coupled device camera or a photomultiplier was used as a detector in all experiments.

Figure 2 shows the FR (Φ_F) in $ErMnO_3$ for a magnetic field $H \parallel z$. At the chosen photon energy (1.35 eV), the sensitivity to H is large due to the proximity of a d-d transition ($^5\Gamma_1 \rightarrow {}^5\Gamma_5$) of the Mn at 1.62 eV [14] without yet being obscured by dichroitic contributions. At 2 K, $\Phi_F(H)$ reveals a typical ferromagnetic hysteresis. The rotation consists of a linear contribution $\Phi_F(H) \propto H$ from the applied field and a ferromagnetic hysteresis $M(H)$ which is due to an Ising-like ferromagnetic magnetization of the two Er sublattices along z. This is confirmed by experiments on the nonmagnetic Y^{3+} sublattice of $YMnO_3$ which shows only a slope, but not a hysteresis of $\Phi_F(H)$ in Fig. 2a. Magnetization measurements [13] point to an antiparallel orientation of the Er(4b) and the Er(2a) spins along z. In total, this leads to ferrimagnetic Er ordering with the uncompensated magnetization along z breaking the geometric frustration of the basal plane.

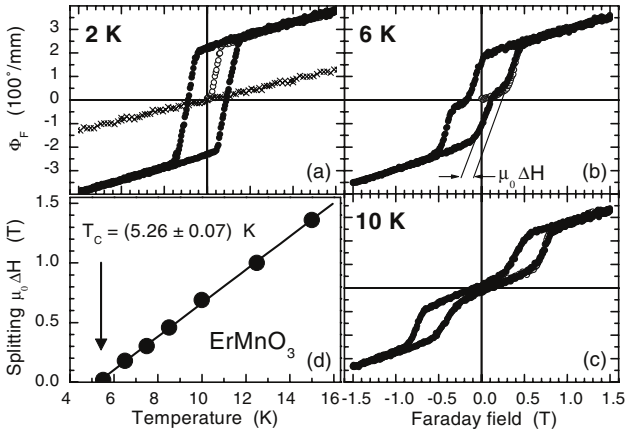

FIG. 2. FR (Φ_F) of $ErMnO_3$ at $E = 1.35$ eV in a magnetic field $H \parallel z$ (open circles: virgin curve). Scaling is the same in panels (a)–(c). The splitting ΔH is defined graphically in (b). Its temperature dependence is shown in (d). For comparison, Φ_F of $YMnO_3$ is shown by crosses in (a).

At 6 and 10 K induced ferrimagnetic ordering is observed which has not been reported before for $ErMnO_3$. It is indicated by a double hysteresis and defines the Curie temperature T_C as the temperature where the spontaneous is replaced by induced ordering. Above T_C the system has to be subjected to the field at least once in order to encounter the long-range ordered phase. Figure 2d shows how the value $T_C = (5.26 \pm 0.07)$ K is determined. Excellent agreement with $T_C = 5.3$ K in [12] confirms the suitability of FR as an optical probe for the magnetic properties of the Er sublattice.

Figure 3a shows the SH intensity for linearly polarized light incident onto a z cut crystal which was cooled to 6 K in zero magnetic field. The SH intensity $I_{\mathrm{SH}} \propto |P_\rho(2\omega, 2k_z)|^2$ was measured in dependence of a magnetic field $H \parallel z$. Around 0.35 T, the SH intensity abruptly drops to zero in the whole investigated spectral range and does not recover upon field removal or reversal. Simultaneously, an irreversible increase of $P_z(2\omega, 2k_x)$ by 50% is observed for the χ_{zzz} component of an x-cut $ErMnO_3$ crystal with $H \parallel z$. (Slightly different critical fields in Figs. 3a and 3b are due to the different growing techniques for the two samples.)

The broad hysteresis of the effect shown in Fig. 3 points to a first-order phase transition. Disappearance of magnetic SH contributions at $P_\rho(2\omega, 2k_z)$ in combination with new magnetically induced contributions at $P_z(2\omega, 2k_x)$ is compatible only with a change from *antiferromagnetic* to

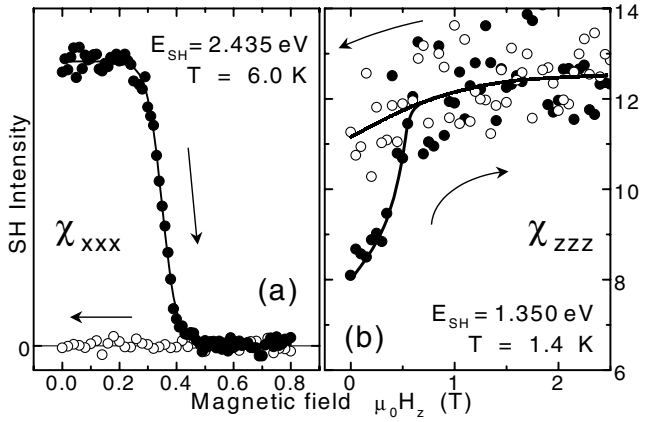

FIG. 3. SH intensity from (a) χ_{xxx} and (b) χ_{zzz} in dependence of a magnetic field $H \parallel z$. The SH energies are determined by the maxima of the corresponding SH spectra [14]. Light is incident along z in (a) and along y in (b). Closed (open) circles and arrows denote the field increasing (decreasing) run. Lines are fits.

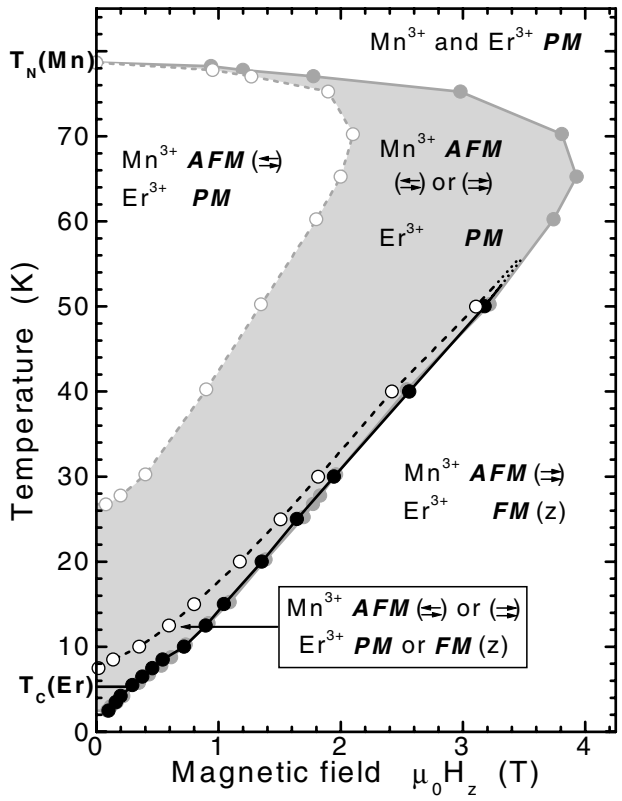

FIG. 4. Phase diagram of $ErMnO_3$ for a magnetic field $H \parallel z$. The right (left) border of the gray region with closed (open) circles and lines in gray marks the reorientation of the Mn lattice in the field increasing (decreasing) run. Closed (open) circles and lines in black mark the transition of the Er lattice into (out of) a single-domain state upon increase (decrease) of H. AFM — antiferromagnetic; FM — ferrimagnetic; PM — paramagnetic; ⇄ (⇉) — antiferromagnetic (ferromagnetic) coupling between adjacent Mn planes along z.

ferromagnetic coupling between adjacent Mn planes along z. This reorientation is quite unexpected since at $B = 0$ the antiferromagnetic coupling is very stable, being the only form of ordering observed in any of the hexagonal manganites, regardless of their structural and magnetic differences. In spite of the reorientation, all Mn spins remain aligned along local y axes. Only for this case a magnetic symmetry $P6_3cm$ leads to new magnetic SH contributions with $\chi_{zzz}^{\mathrm{mag}} \neq 0$ which interfere with the already existing nonmagnetic contributions, thus leading to the observed increase of SH intensity in Fig. 3b [9]. Therefore, the relative orientation of Mn spins in *adjacent basal planes* is reversed while the order *inside the basal plane* is left unchanged. This is in agreement with the fact that the interplane correlations are much weaker than the in-plane correlations. For the same reason, ferromagnetic ordering of all Mn spins along z can be excluded as explanation for the result in Fig. 3. As expected, a 7 T field applied *in* the basal plane could *not* change the magnetic structure of $ErMnO_3$.

Because of the subtlety of the phase transition which affects only the third-order magnetic exchange in one dimension, it is difficult to be observed with conventional methods probing magnetism. The magnetic susceptibility of the Mn sublattice should be the same for antiferromagnetic or ferromagnetic coupling between adjacent planes. The transition is further obscured by the simultaneous ordering of the Er sublattice. Note that the FR in Fig. 2 and, thus, the magnetization measurements indicate only ordering of the Er spins while being insensitive to the hidden transition of the Mn lattice. It is revealed only because SHG is sensitive to subtle differences in the magnetic structure without being hampered by the Er ordering.

Temperature dependent measurements of the FR and the SHG as shown in Figs. 2 and 3 reveal the phase diagram for the magnetic sublattices of Er and Mn as shown in Fig. 4. The data points for Er were derived from the turning point of the virgin curve of $\Phi_F(H)$. The data points for Mn were derived from the turning point of the Boltzmann function fitting the field dependence of the SHG in Fig. 3a. All values except that at T_N were gained from field increasing and decreasing runs at a fixed temperature. Temperature dependent measurements at selected magnetic fields revealed identical phase boundaries for Mn within a margin of ± 1 K. Up to about 80% of T_N, the critical field for the magnetic phase transitions increases approximately linearly with T. Because of a hysteresis of up to 2 T, the high-field state of the Mn lattice is maintained persistently below 27 K. Close to T_N, backbending of the hysteresis occurs until the critical field reaches zero at T_N. Note that below 1.5 K the phase transition of the Mn lattice occurs spontaneously.

The most remarkable feature of Fig. 4 is the coincidence of phase boundaries for the (re-) ordering of the Er and the Mn spins upon field increase. Obviously, the magnetization of the Er lattice *perpendicular* to the direction of the Mn spins triggers the antiferromagnetic-to-ferromagnetic phase transition of the Mn lattice. The microscopic origin of this unusual behavior can be understood by calculating the anisotropic exchange interaction between the Mn and

Er sublattices. The interaction is given by

$$H_{\mathrm{ex}} = \sum_{k=3m,3} \sum_{i_k=1}^{2(k=3m)\;\;4(k=3)} \sum_{j=1}^{6} \vec{S}^{\mathrm{Er}^k(i_k)} \hat{A}^{k,i_k,j} \vec{S}^{\mathrm{Mn}(j)} \quad (3)$$

with $\vec{S}^{\mathrm{Er}}$ and $\vec{S}^{\mathrm{Mn}}$ as spin vectors and $\hat{A}$ as the 3×3 exchange matrix. The summation in k includes the two Er sites with 3 and $3m$ symmetries. The summation in i_k includes all Er ions at k sites in the unit cell. There are two ions if $k = 3m$ and four ions if $k = 3$. The summation in j includes the six Mn ions neighboring each Er ion. Exchange paths other than those shown in Fig. 1 can be neglected due to large distances between the ions or unfavorable bond angles [15].

With $\vec{S}^{\mathrm{Er}} = (0, 0, \pm S_z^{\mathrm{Er}})$ and $\vec{S}^{\mathrm{Mn}} = (S_x^{\mathrm{Mn}}, S_y^{\mathrm{Mn}}, 0)$, the only relevant tensor components of any tensor $\hat{A}$ are A_{zx} and A_{zy}. The exchange contributions from the nearest Mn neighbors below each Er ion at a site k are equal and denoted by $\hat{A}^k$. There are six such tensors if $k = 3m$ and twelve if $k = 3$. The same arguments hold for the contributions from the nearest Mn neighbors above each Er ion. They are denoted by $\underline{\hat{A}}^k$. One finds $\vec{S}^{\mathrm{Mn}} = S^{\mathrm{Mn}}(0, 1, 0)$ for Mn ions 1, $1'$, $\underline{1}$, $\underline{1}'$; $\vec{S}^{\mathrm{Mn}} = S^{\mathrm{Mn}}(-\sqrt{3}/2, -1/2, 0)$ for Mn ions 2, $\underline{2}$; and $\vec{S}^{\mathrm{Mn}} = S^{\mathrm{Mn}}(\sqrt{3}/2, -1/2, 0)$ for Mn ions 3, $3'$, $\underline{3}$, $\underline{3}'$ in Fig. 1 for antiparallel coupling between basal Mn planes. For parallel coupling, the spins of ions labeled with an underbar have to be reversed. The rare-earth spin for ferrimagnetic ordering of the Er sublattices is given by $\vec{S}^3 = -\vec{S}^{3m} = (0, 0, S^{\mathrm{Er}})$.

With these relations one finds that as a consequence of the antiferromagnetic coupling between basal Mn planes the exchange contributions from ions in the lower half of the unit cell (labeled with an underbar) cancel out those from the ions in the upper half (no bar) which leads to $H_{\mathrm{ex}}(\rightleftarrows) = 0$. However, for ferromagnetic coupling, one gets

$$H_{\mathrm{ex}}^{\ell}(\rightrightarrows) = 6\ell S^{\mathrm{Er}} S^{\mathrm{Mn}} [(A_{zy}^{3m} + \underline{A}_{zy}^{3m}) + (A_{zy}^{3} + \underline{A}_{zy}^{3})], \quad (4)$$

where $\ell = \pm 1$ denotes the two 180° domains of the planar triangular ordering. A lowering of the ground state for one of the no longer degenerate 180° domains of the Mn lattice is thus expected. Therefore, the reorientation of the Mn lattice is observed upon ferrimagnetic ordering of the Er^{3+} spins along z. The applied field $H \parallel z$ increases the alignment of the Er^{3+} spins along z, thus strengthening the exchange with the Mn^{3+} spins and supporting the phase transition. Once the high-field state has been encountered, it is stabilized by the Mn-Er exchange even in the absence of long-range Er ordering which leads to the broad hysteresis in Fig. 4.

A phase diagram similar to that shown in Fig. 4 was observed in all hexagonal $R\mathrm{MnO_3}$ samples with a partially filled $4f$ shell (R = Ho, Er, Tm, Yb), but not in the compounds with R = Y, Sc, Lu. Along with the comparison in Fig. 2a, this stresses the importance of a strong $R(4f)$ − Mn($3d$) exchange. A phase transition at zero magnetic field was observed only in $HoMnO_3$ and $ErMnO_3$, the compounds with the largest effective magnetic moment of the rare-earth ion.

In conclusion, the combination of FR and SHG as complementary optical techniques was used to reveal a hidden first-order magnetic phase transition in hexagonal $ErMnO_3$. The spontaneous or field induced transition roots in the breaking of inter- and intrasublattice frustration by a spontaneous or induced Ising-like Er magnetization which is oriented perpendicular to the plane of the dominating superexchange between the Mn ions. This leads to a situation in which the much weaker anisotropic third-order and Er-Mn exchange processes dominate the magnetic properties of the system. The observed phase transition demonstrates in an impressive way how multiple disorder arising from magnetic frustration on several levels finally leads to a highly ordered and correlated state with interesting perspectives for a better understanding of magnetic frustration and its consequences.

The authors thank D. Fröhlich for his continuous interest and support, K. Kohn for samples and sending his results prior to publication, and the Russian Foundation for Basic Research, the Deutsche Forschungsgemeinschaft, and the A.-von-Humboldt-Stiftung for financial support.

*Email address: fiebig@janeway.physik.uni-dortmund.de

[1] M. F. Collins and O. A. Petrenko, Can. J. Phys. **75**, 605 (1997).
[2] H. Kawamura, J. Phys. Condens. Matter **10**, 4707 (1998).
[3] H. Oshima, M. Nakamura, and K. Miyano, Phys. Rev. B **63**, 75 111 (2001).
[4] V. P. Plakhty *et al.,* Phys. Rev. Lett. **85**, 3942 (2000).
[5] M. Tissier, B. Delamotte, and D. Mouhanna, Phys. Rev. Lett. **84**, 5208 (2000).
[6] J. E. Greedan *et al.,* J. Solid State Chem. **116**, 118 (1995).
[7] E. F. Bertaut, M. Mercier, and R. Pauthenet, Phys. Lett. **5**, 27 (1963).
[8] W. C. Koehler, H. L. Yakel, E. O. Wollan, and J. W. Cable, in *Proceedings of the 4th Conference on Rare-Earth Research, Phoenix, Arizona, 1964* (Gordon and Breach, New York, 1965), p. 63; Phys. Lett. **9**, 93 (1964).
[9] M. Fiebig *et al.,* Phys. Rev. Lett. **84**, 5620 (2000).
[10] This corresponds to a parallel orientation of neighboring spins S and $\underline{S}$ in Fig. 1 and in Ref. [9]. However, with the $\underline{6}(0, 0, c/2)$ correspondence between the two halfs of the unit cell and for the Mn—O—O—Mn exchange, the present terminology is physically more reasonable.
[11] R. Pauthenet and C. Veyret, J. Phys. (Paris) **31**, 65 (1970). (Curie temperatures are incorrectly listed due to a misprint.)
[12] N. Iwata and K. Kohn, Ferroelectrics **219**, 161 (1998); J. Phys. Soc. Jpn. **67**, 3318 (1998). (The results for $ErMnO_3$ and $HoMnO_3$ have to be exchanged.)
[13] H. Sugie, N. Iwata, and K. Kohn (unpublished).
[14] C. Degenhardt *et al.,* Appl. Phys. B **73**, 139 (2001).
[15] K. Kritayakirana, P. Berger, and R. V. Jones, Opt. Commun. **1**, 95 (1969).